

Methods for Producing Scaffold-Free Engineered Cartilage Sheets from Auricular and Articular Chondrocyte Cell Sources and Attachment to Porous Tantalum

G. Adam Whitney,¹⁻³ Hisashi Mera,³ Mark Weidenbecher,⁴ Amad Awadallah,⁵ Joseph M. Mansour,^{2,6} and James E. Dennis¹⁻³

Abstract

Scaffold-free cartilage engineering techniques may provide a simple alternative to traditional methods employing scaffolds. We previously reported auricular chondrocyte-derived constructs for use in an engineered trachea model; however, the construct generation methods were not reported in detail. In this study, methods for cartilage construct generation from auricular and articular cell sources are described in detail, and the resulting constructs are compared for use in a joint resurfacing model. Attachment of cartilage sheets to porous tantalum is also investigated as a potential vehicle for future attachment to subchondral bone. Large scaffold-free cartilage constructs were produced from culture-expanded chondrocytes from skeletally mature rabbits, and redifferentiated in a chemically-defined culture medium. Auricular constructs contained more glycosaminoglycan (39.6 ± 12.7 vs. 9.7 ± 1.9 $\mu\text{g}/\text{mg}$ wet weight, mean and standard deviation) and collagen (2.7 ± 0.45 vs. 1.1 ± 0.2 $\mu\text{g}/\text{mg}$ wet weight, mean and standard deviation) than articular constructs. Aggregate modulus was also higher for auricular constructs vs. articular constructs (0.23 ± 0.07 vs. 0.12 ± 0.03 MPa, mean and standard deviation). Attachment of constructs to porous tantalum was achieved by neocartilage ingrowth into tantalum pores. These results demonstrate that large scaffold-free neocartilage constructs can be produced from mature culture-expanded chondrocytes in a chemically-defined medium, and that these constructs can be attached to porous tantalum.

Key words: biomaterials; cell culture; regeneration; tissue engineering

Introduction

DIVERSE APPROACHES ARE BEING EXPLORED to regenerate cartilage. In the majority of cartilage tissue engineering applications, a carrier or scaffold material is employed to allow 3D attachment of cells, shaping of constructs, and in some cases growth factor delivery.¹⁻³ Alternatively, constructs can be produced scaffold-free by seeding cells at high densities such that cells are layered on top of each other. In such constructs, the scaffold is the natural extracellular material fabricated by the chondrocytes themselves.^{4,5} The fabrication of scaffold-free cartilage may more closely mimic embryonic development, where a high cell density state in the developing anlagen precedes matrix production.⁶

Scaffold-free methods have been described in various platforms ranging from spheroid aggregates^{5,7,8} to cartilage

sheets. Scaffold-free cartilage sheet generation has been described from rat,⁹ bovine,¹⁰⁻¹² goat,¹³ pig,¹⁴ rabbit,^{15,16} and human⁴ articular chondrocyte cell sources, and human mesenchymal stem cell sources.¹⁷ We previously reported a simple serum-free differentiation method for scaffold-free engineered cartilage generation from rabbit auricular chondrocytes for use in engineered trachea and laryngotracheal reconstruction models.^{18,19} We are now developing our cartilage engineering techniques for use in arthroplasty models. Compositional differences in native articular and auricular cartilage suggest that articular chondrocyte-derived constructs may perform better in joint repair. However, generation of scaffold-free engineered cartilage by articular chondrocytes from skeletally mature rabbits in a chemically-defined medium has not been reported. Additionally, no effective method to attach scaffold-free constructs to the subchondral bone has been

Departments of ¹Biomedical Engineering, ²Orthopaedics, ⁵Biology, and ⁶Mechanical and Aerospace Engineering, Case Western Reserve University, Cleveland, Ohio.

³Hope Heart Matrix Biology Program, Benaroya Research Institute, Seattle, Washington.

⁴Department of Otolaryngology, University Hospitals, Cleveland, Ohio.

demonstrated. Attachment to the bone will be necessary for stability of the implant and for the proper transfer of joint forces from cartilage to the underlying bone. To overcome the attachment problem, we are currently developing methods to integrate porous tantalum into our cartilage sheets due to its high porosity and established use in clinical orthopedics.^{20–22} Successful integration could allow immediate fixation to the bone, and allow bone ingrowth *in vivo*.

Here, we demonstrate techniques to generate scaffold-free cartilage from articular cell sources, and compare these constructs to auricular chondrocyte-derived constructs with respect to their composition and mechanical properties. In addition, we demonstrate a methodology to integrate scaffold-free cartilage sheets with porous tantalum as a potential vehicle for bone attachment.

Materials and Methods

Scaffold-free cartilage generation

Isolation and expansion of chondrocytes. Cartilage was harvested from the ears (auricular cartilage) and knees (articular cartilage) of adult male New Zealand White rabbits under sterile conditions, and the perichondrium was removed from the auricular cartilage. Cartilage was cut into $\sim 1 \text{ mm}^3$ pieces and sequentially digested at 37°C on a nutating rocker in 660 units/mL testicular hyaluronidase (H-3506; Sigma-Aldrich, St. Louis, MO) in Dulbecco's modified Eagle's medium (DMEM) for 15 min, trypsin/EDTA (25200-072; Invitrogen, Carlsbad, CA) for 30 min, and 580 units/mL collagenase Type II (CLS 2; Worthington Biochemical Corp, Lakewood, NJ) overnight in DMEM (11885; Invitrogen). Chondrocytes were then passed through a 70- μm filter, resuspended in DMEM, and centrifuged at 690g for 10 min. Supernatant was removed and cells were resuspended in DMEM supplemented with 10% fetal bovine serum (FBS) (lot #1256415; Invitrogen). Chondrocytes were plated at 5.7×10^3 cells/cm² in cell culture flasks (431080; Corning, Lowell, MA) and culture-expanded in 10% FBS in DMEM until confluent, and then trypsinized. Cells were then subcultured for two passages to obtain the large number of cells required in the large format constructs described below.

Scaffold-free construct formation. Auricular cartilage constructs were formed by the method reported by Gilpin et al.,¹⁹ wherein passaged chondrocytes suspended in the chondrogenic medium were seeded into custom biochambers comprised of two compartments with porous (10 μm pore diameter) polyester membranes (PET1009030; Sterlitech, Kent, WA) (Fig. 1A) separating the compartments (Fig. 1A–C). Articular chondrocytes were seeded at a density of 3.125×10^6 cells/cm², while auricular chondrocytes were seeded at 1.875×10^6 cells/cm². These seeding densities were chosen because they were the maximum allowable without inducing necrosis (Fig. 1D), and it was noted during preliminary studies that fewer cells resulted in thinner, less stiff constructs. Biochambers produced $\sim 4 \text{ cm} \times 4 \text{ cm}$ cartilage sheets (Fig. 1E). These large surface areas enable clinical reconstructions such as in the engineered trachea model reported previously.¹⁸ Biochambers were formed by sandwiching the porous membrane between the two stainless steel plates that comprise the biochamber, then proceeding

with assembly as detailed in Figure 2A. This assembly was then placed into a 10-cm tissue culture dish. Assembled biochamber dimensions are shown in Figure 2B.

During culture, the chondrogenic medium was exchanged every 2 days in both the inner and outer compartments (Fig. 1A, C) for articular constructs. Auricular constructs required the inner compartment medium to be changed every day due to more rapid acidification of the culture medium, indicating a higher metabolic rate. During the first 4 days of culture, care should be taken when feeding the constructs because they are susceptible to premature detachment, and if detached will contract to less than half their original size. To prevent detachment, the culture medium can be dispensed onto the metal frame and allowed to flow into the inner compartment of the biochamber, rather than dispensing directly onto the tissue. The chondrogenic defined medium consists of DMEM with 4.5 g/L glucose supplemented with 1% ITS+ premix (354352; BD Biosciences, San Jose, CA), 10^{-7} M dexamethasone (D4902; Sigma-Aldrich), 0.13 mM L-ascorbate-2-phosphate (013-12061; Wako Chemicals, Richmond, VA), and 1:100 dilutions of GlutaMAX, nonessential amino acids, 100 mM sodium pyruvate, and Antibiotic-Antimycotic (35050079, 11140-076, 11360 and 15240112; Invitrogen).

Neocartilage was removed from the porous membrane between 3 and 4 weeks, then cultured in free-float culture with the chondrogenic medium until a total culture time of 8 weeks was reached. The membrane-attached culture period was modified from the methods reported by Gilpin, et al.¹⁹ because at 3 weeks, removal of the articular constructs from the membrane was not possible without damaging the constructs. The free-float culture was necessary for articular constructs to gain sufficient mechanical properties to be handled. During the free-floating phase, the chondrogenic medium was exchanged at least twice per week by removing all the medium in the tissue culture dish and replacing it with $\sim 25 \text{ mL}$ of fresh medium.

Construct characterization

Histological characterization. Tissue samples were taken during and at the end of tissue culture and fixed in 10% formalin overnight, dehydrated in sequential ethanol baths from 70% to 100% ethanol, then embedded in paraffin, and sectioned to 7- μm -thick cross sections. Sections were stained with Safranin O and fast green to visualize glycosaminoglycan (GAG) and cellular components, respectively. Thickness measurements were made on stained tissue sections in NIH ImageJ (NIH, Bethesda, MD) by taking the average of three measurements of one section for each specimen tested.

Biochemical composition and structure. We have modified previously described methods for measuring DNA,²³ GAG,²⁴ and hydroxyproline (HYP), an indicator of total collagen content.^{25,26} These modifications make it possible to measure water content, solid content, DNA, GAG, and HYP from a single sample digestion. Immediately after harvest, samples were lightly blotted on filter paper, and wet weights obtained. Samples were then lyophilized overnight and dry weights obtained, and solid content was calculated as a ratio of the solid (dry) to total (wet) weight. Samples were then digested in 200 μL papain solution adjusted to pH 6.5

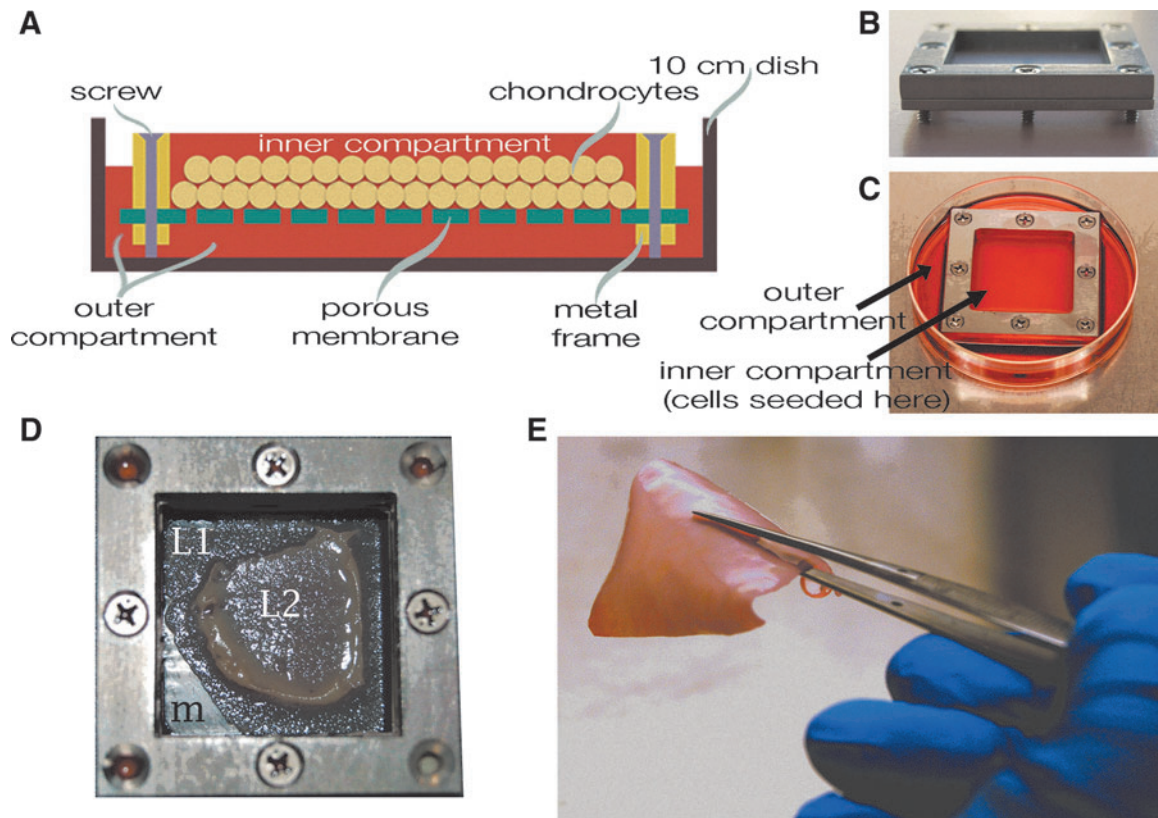


FIG. 1. Generation of scaffold-free cartilage constructs. A custom biochamber (A–C), consisting of an inner and outer compartment, was used to generate scaffold-free cartilage. (A) A representative drawing of a biochamber. Within the inner compartment, chondrocytes attach to a porous membrane, which allows the attached surface of the neocartilage to access the culture medium in the outer compartment, and the free surface to access the medium in the inner compartment. (B) An image of the inner compartment of the biochamber. Screws, which hold the porous membrane sandwiched between two metal plates also elevate the frame so that the culture medium can access the underneath of the porous membrane. (C) An image of the completed biochamber. The frames are placed into a 10-cm culture dish, which forms the outer compartment of the biochamber. (D) A representative image of the necrosis that occurs when constructs are initiated with too many cells. The membrane can be seen (m), as well as two layers of cartilage, which are separating due to necrosis, a layer attached to the membrane (L1), and a layer, which has detached and contracted (L2). (E) A representative image of the scaffold-free constructs produced in these biochambers with the recommended cell seeding density.

(25 $\mu\text{g}/\text{mL}$ papain, 2 mM cysteine, 50 mM sodium phosphate, and 2 mM EDTA [all from Sigma-Aldrich]) at 65°C for 3 h. After digestion, a 100 μL aliquot was taken for the collagen assay, and the remaining 100 μL was used for the DNA and GAG assays.

GAG/DNA aliquots were incubated with 200 μL 0.1 M sodium hydroxide (NaOH) for 30 min at room temperature, treated with 200 μL of neutralizing solution (5 M sodium chloride and 100 mM disodium phosphate dibasic, pH 7.2, then brought to a final concentration of 0.1 normality [N] hydrochloric acid). Calf thymus DNA standards were prepared from blanks treated identically to samples. Fluorescence at 465 nm with excitation at 340 nm was measured in triplicates containing 75 μL of 1 mg/mL Hoeschst 33258 diluted at 1:1500 in water and 75 μL of sample or standard on a 96-well plate. The same solution used to quantify DNA was then used to quantify GAG in a spectrophotometer by Safranin O absorbance, as previously described.²⁴

Collagen content was quantified by a HYP assay. Papain-digested (see above) HYP aliquots were hydrolyzed with 1 mL of 6 N HCl at 110°C in a fume hood overnight. Then,

sample vials were opened and HCl was evaporated at 65°C until dry. Samples were resuspended in 200 μL of water and a 100 μL aliquot was taken for assay. To the 100 μL aliquot, 100 μL of 0.15 copper sulfate and 100 μL of 2.5 N NaOH were added, then samples were incubated at 40°C for 5 min, then 100 μL of 6% hydrogen peroxide was added, followed by an additional 10-min incubation at 40°C before cooling to room temperature. 400 μL of 3 N sulfuric acid, and 200 μL of 5% p-dimethyl-amino-benzaldehyde were then added to each sample, followed by incubation at 70°C for 16 min, and cooling to room temperature. Absorbance was read at 492 nm for 200 μL of each sample in triplicate on a 96-well plate. Standards were prepared from purified hydroxyproline (H5877; Sigma-Aldrich). Samples with HYP values outside the range of the standard curve were diluted and retested using the remaining 100 μL from the original sample. GAG and HYP values were normalized to DNA, wet and dry weights, and cellularity was estimated from the DNA content and wet weight assuming 7.7×10^{-12} g DNA/chondrocyte.²⁷ For one articular construct, dry weight of test samples was calculated from

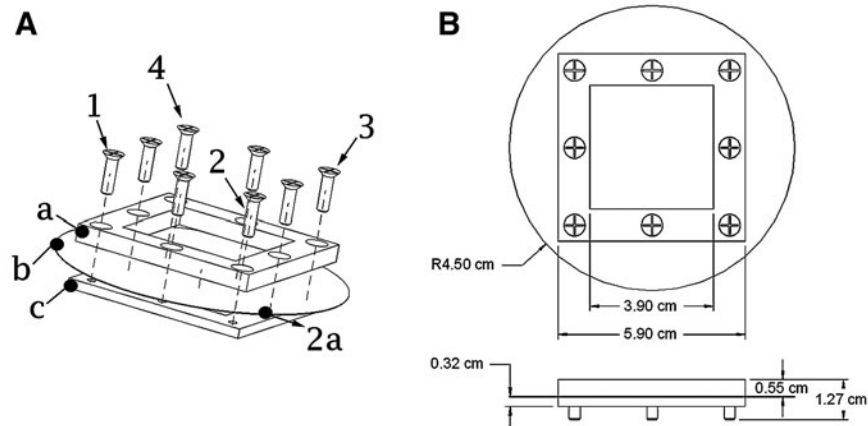


FIG. 2. Biochamber assembly. **(A)** To assemble biochambers, the porous membrane (b) is sandwiched between the two metal frames (a, c) and corner screws (1–4) are inserted and lightly tightened. As each is tightened, the membrane is pulled along the vector between it and the previous screw (2a), as shown for the second screw (2). After lightly tightening corner screws, the middle screws are tightened while putting tension on the membrane, being careful to not create wrinkles in the membrane. All screws are then tightened. The excess membrane is then removed from the outside of the chamber. **(B)** Schematic showing the final dimensions of the assembly, before removal of the excess membrane. The circle with R4.5 cm is the porous membrane.

the solid content of representative samples from the same sheet.

Mechanical characterization. Mechanical properties of the extracellular matrix (ECM) (Poisson's ratio and aggregate modulus) were determined by indentation testing as previously described.^{28,29} Sample thickness was measured using a custom device that detects contact of a micrometer tip with cartilage by monitoring changes in resistance to the flow of a small electrical current. For testing, samples were adhered to a solid substrate using cyanoacrylate. This maintains the no-slip and no-fluid-flow boundary conditions at the cartilage–substrate interface, which are assumed in data processing to obtain mechanical properties. During testing, samples were bathed in phosphate-buffered saline. A cylindrical porous stainless steel tip with a diameter of 1.07 mm was used to apply tare and test loads to samples, and displacement was measured using a linear variable transducer. After displacement reached equilibrium under the tare load, the test load was applied and displacement over time was recorded. A 1 g test load was chosen, to limit the engineered cartilage compressive strain to ~20%. Aggregate modulus, shear modulus, and permeability were determined as parameters of biphasic stress-strain equations fit to test load–displacement data as described by Mak et al. and Mow et al.^{28,29}

Porous tantalum integration

To integrate porous tantalum and constructs, we used a modified biochamber, with multiple wells (Fig. 3A, B). Porous membranes were coated with fibronectin, and then the chondrogenic culture medium was dispensed in the tissue culture dish (outer compartment) until the medium began to enter the wells of the biochamber through the porous membrane (Fig. 3C-1). Adding the medium to the outside biochamber before seeding cells is necessary to avoid trapping air underneath the membrane. Auricular chondrocytes suspended in the chondrogenic culture medium were then

seeded at 1.875×10^6 cells/cm² (Fig. 3C-2). Porous tantalum (Zimmer, Warsaw, IN) was then placed on top of the neocartilage 2 days later (Fig. 3C-3); preliminary studies indicated that if added at later time points, the constructs were less likely to attach. Chondrocytes from two rabbits were used to produce a total of four constructs.

Statistical analysis

The analysis was performed in PRISM (GraphPad, La Jolla, CA) with significance defined as $p < 0.05$. Data are presented as mean and standard deviation. For composition and mechanical characterization, two or more samples per construct were analyzed, and the mean value for each construct was calculated. For mechanical properties and thickness tests, a two-tailed Student's *t*-test was used to compare auricular and articular constructs. In mechanical property comparisons, there was an $n=4$ of articular constructs and an $n=3$ of auricular constructs. In thickness comparisons, articular constructs had an $n=5$ and auricular constructs an $n=3$. For compositional assays, the one-way analysis of variance with the Tukey *post hoc* analysis was used to compare auricular constructs, articular constructs, and native cartilage. In composition comparisons, there was an $n=4$ of articular constructs, $n=3$ for auricular constructs, and native articular cartilage had an $n=6$.

Results

Scaffold-free cartilage generation

Constructs folded on themselves when handled immediately after removal from the culture biochamber (Fig. 4A), but retained their original size. At the end of the free-float culture period, auricular sheets maintained sheet geometry when handled (Fig. 4B), while some constructs formed with articular chondrocytes still folded on themselves. The bioreactor configuration used in this study allowed cartilage to access nutrients on both the top and bottom surfaces, making the high seeding densities possible. These constructs

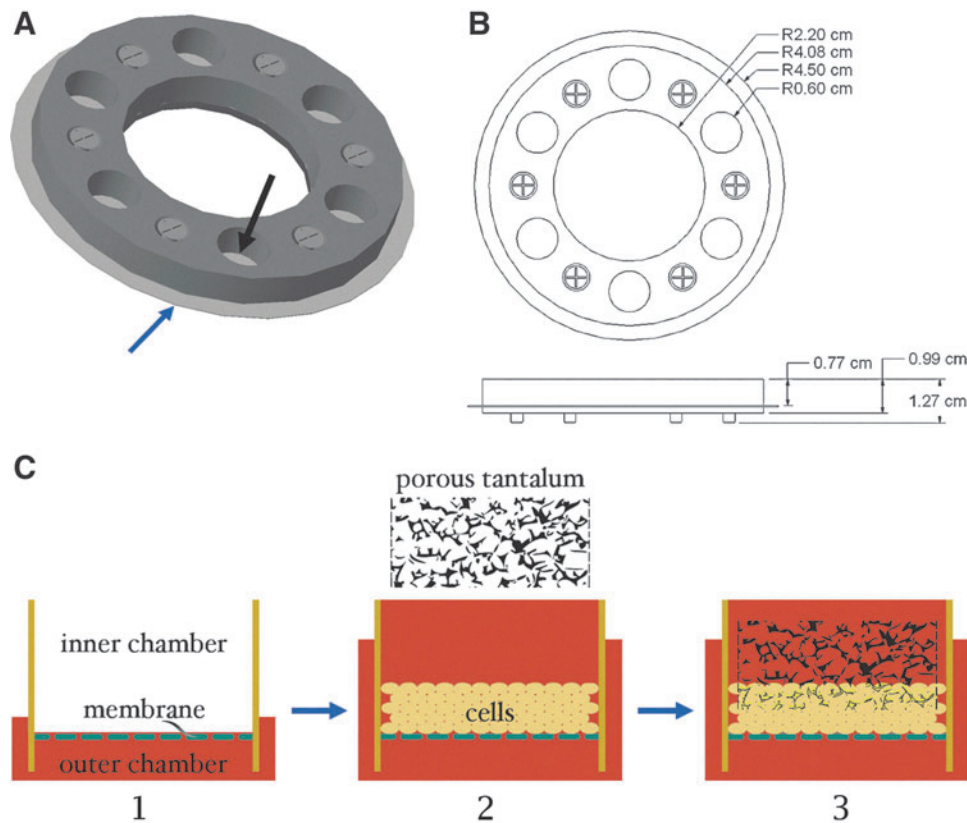


FIG. 3. Generation of cartilage–tantalum composite. **(A)** Rendering of the inner compartment of a multiwell biochamber used to generate the constructs. The black arrow indicates one well, and the blue arrow indicates the porous membrane, which forms the bottom of the well. This component is placed into a 10-cm culture dish to complete the biochamber, as with the single-well biochamber (Fig. 1). **(B)** Schematic showing the dimensions of the multiwell biochamber. **(C)** Process flow for cartilage–tantalum composite generation. The culture medium is first added to the tissue culture dish (outer compartment) until the culture medium begins to enter the wells (inner compartment) through the porous membrane (1). Cell suspension is then added to the wells, using enough culture medium to fill the well (9 mL). Extra culture medium is then added to the culture dish until the medium is ~5 mm from the top of the metal frame (2). Constructs are cultured for 2 days, then porous tantalum is placed on top of the developing neocartilage, and cartilage grows through the interconnected pores (3).

are shown (Fig. 4A–D) next to those produced by a previous configuration, which did not allow such high seeding densities¹⁸ (Fig. 4E, F).

Construct characterization

Histological characterization. Images from histologic sections of auricular and articular constructs showed mostly uniform Safranin O staining of the ECM, with less intense staining at the upper surface and flattened cells at both the upper and lower surfaces (Fig. 4C, D). In addition, it was noted that while auricular constructs were initiated with fewer cells than articular constructs, at harvest they were thicker than articular constructs ($560 \pm 12 \mu\text{m}$ compared with $277 \pm 95 \mu\text{m}$, $p < 0.05$). Representative images are shown in Figure 4C and D.

Biochemical composition and structure. The modification to include HYP quantification along with the previously reported GAG and DNA quantification methods²³ from a single-tissue specimen was shown to give comparable results for native articular cartilage HYP reported in literature.³⁰ The

biochemical characterization of our articular constructs using these methods showed the GAG and HYP content to be about one-half and one-fourth that of native rabbit articular cartilage, respectively (Fig. 5A, B). Auricular constructs contained nearly twice the amount of GAG as native articular cartilage on a DNA and wet weight basis (Fig. 5A), but about one-third the amount of HYP (Fig. 5B). Cellularity of both constructs was not statistically different compared to each other and compared to native articular cartilage (Fig. 5C). Solid content was significantly lower in engineered constructs as compared to native articular cartilage (Fig. 5D).

Mechanical characterization. Aggregate modulus and Poisson's ratio were significantly lower for articular constructs than for auricular constructs (Fig. 5E), indicating that auricular constructs were stiffer and less compressible.

Porous tantalum integration

Four of four neocartilage constructs attached to the porous tantalum. Constructs remained attached to tantalum when handled after 4 weeks of culture (Fig. 6A). Staining with

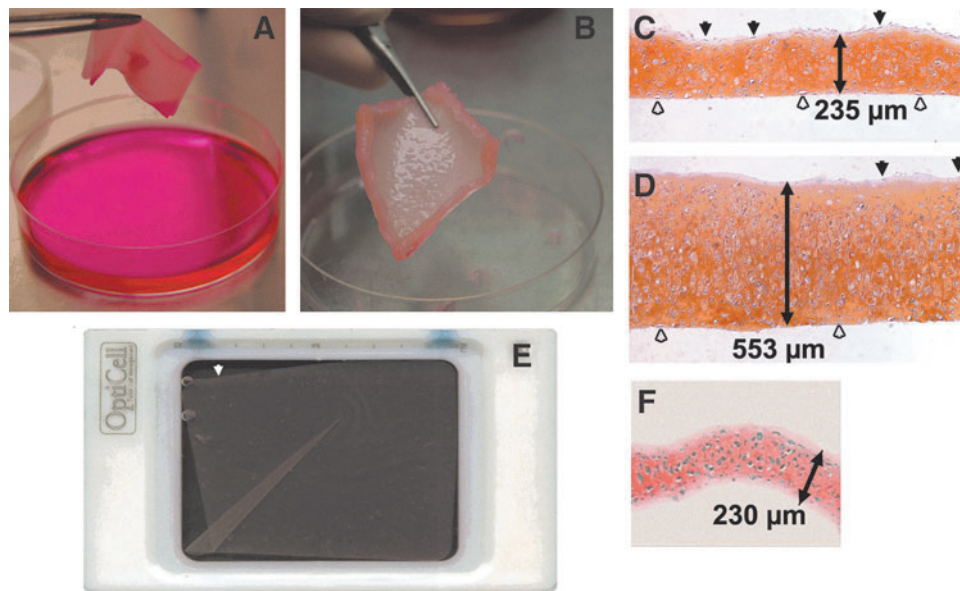


FIG. 4. Scaffold-free neocartilage. **(A)** Image of articular neocartilage after 8 weeks of culture. **(B)** Image of auricular neocartilage after 8 weeks of culture. **(C–D)** Safranin O-stained histological micrographs of **(A, B)**, respectively. Safranin O staining corresponds to glycosaminoglycan (GAG) content. White arrowheads show the surface, which was adjacent to the membrane during the culture, and black arrowheads show the free surface. **(E)** Opticell™ chamber and developing neocartilage. An edge of the neocartilage is shown by a white arrowhead. **(F)** Safranin O-stained cross section of auricular neocartilage produced in an Opticell chamber.

toluidine blue indicated a GAG-rich matrix (Fig. 6B), which attached to the porous tantalum by neocartilage growth through pores in the tantalum (Fig. 6C). A surface layer $\sim 175 \mu\text{m}$ thick remained on the surface of the tantalum (Fig. 6B).

Discussion

Criteria for growing clinically useful scaffold-free engineered cartilage differ by application, but for greatest utility for implantation, cells would be harvested from skeletally mature sources, be cultured in chemically-defined medium, and be capable of generating constructs of a comparable size to adult human anatomical structures, such as the tibial plateau, tracheal segments, nasal septum, or the pinna of the ear. Although rabbit models have frequently been used for analyses of *in vitro* and *in vivo* cartilage and bone repair,^{31–34} no method for scaffold-free rabbit articular cartilage generation meeting these criteria has been described. In these studies, serum-supplemented medium is used during the expansion phase, but we are able to drive redifferentiation with chemically-defined medium. Other than serum supplementation during expansion, the engineered cartilage produced here meet the criteria above. As we develop this technology for application to joint resurfacing for osteoarthritis, we compared constructs of articular and auricular origin.

ECM production and stiffness of articular and auricular chondrocyte-derived constructs have been directly compared and reported for systems employing scaffolds for cartilage engineering,²³ and in this study, we obtained comparable results using a scaffold-free system. Specifically, auricular constructs produced more ECM per cell, were stiffer, and less compressible than articular constructs (Fig. 5). Auricular constructs also required fewer cells to produce, yet resulted in

thicker constructs due to production of more ECM per cell. Compared to constructs reported in the literature, the articular construct composition and aggregate modulus were similar to other scaffold-free constructs reported.^{12,15,16} Auricular construct aggregate modulus was comparable to values we have reported previously using this same technique.¹⁹ We have not found aggregate modulus reported for scaffold-free auricular constructs grown using other techniques. In comparison to auricular constructs employing scaffolds, the constructs in this study were about 100% more stiff than 6-week rabbit constructs employing Hyalograft-C™ scaffold²³ (Fidia Advanced Biopolymers, Terme, Italy) and 180% stiffer than 12-week porcine auricular constructs employing hyaluronic acid hydrogels.³⁵ Both articular and auricular constructs were about one-fourth the stiffness reported in literature for their respective native cartilage counterparts.³⁶ The increased ECM content and stiffness of auricular constructs might indicate that they would perform better under the high-load environment of a load-bearing joint. To our knowledge, functional comparison between auricular and articular scaffold-free engineered constructs has not been performed, but would be useful to determine if auricular constructs could be used in the joint environment.

Successful *in vivo* implantation of either articular or auricular constructs within a joint will be dependent on a method to attach cartilage constructs to an underlying bone. Attachment may be possible by using a porous interface, to which both cartilage and bone can integrate, while still allowing nutrient and waste transport. One such material with a pre-established history in orthopedics is porous tantalum.³⁷ Integration of porous tantalum into engineered cartilage constructs employing scaffolds has been described;^{38–40} although we know of no prior description of integration of porous tantalum and scaffold-free engineered cartilage. The method

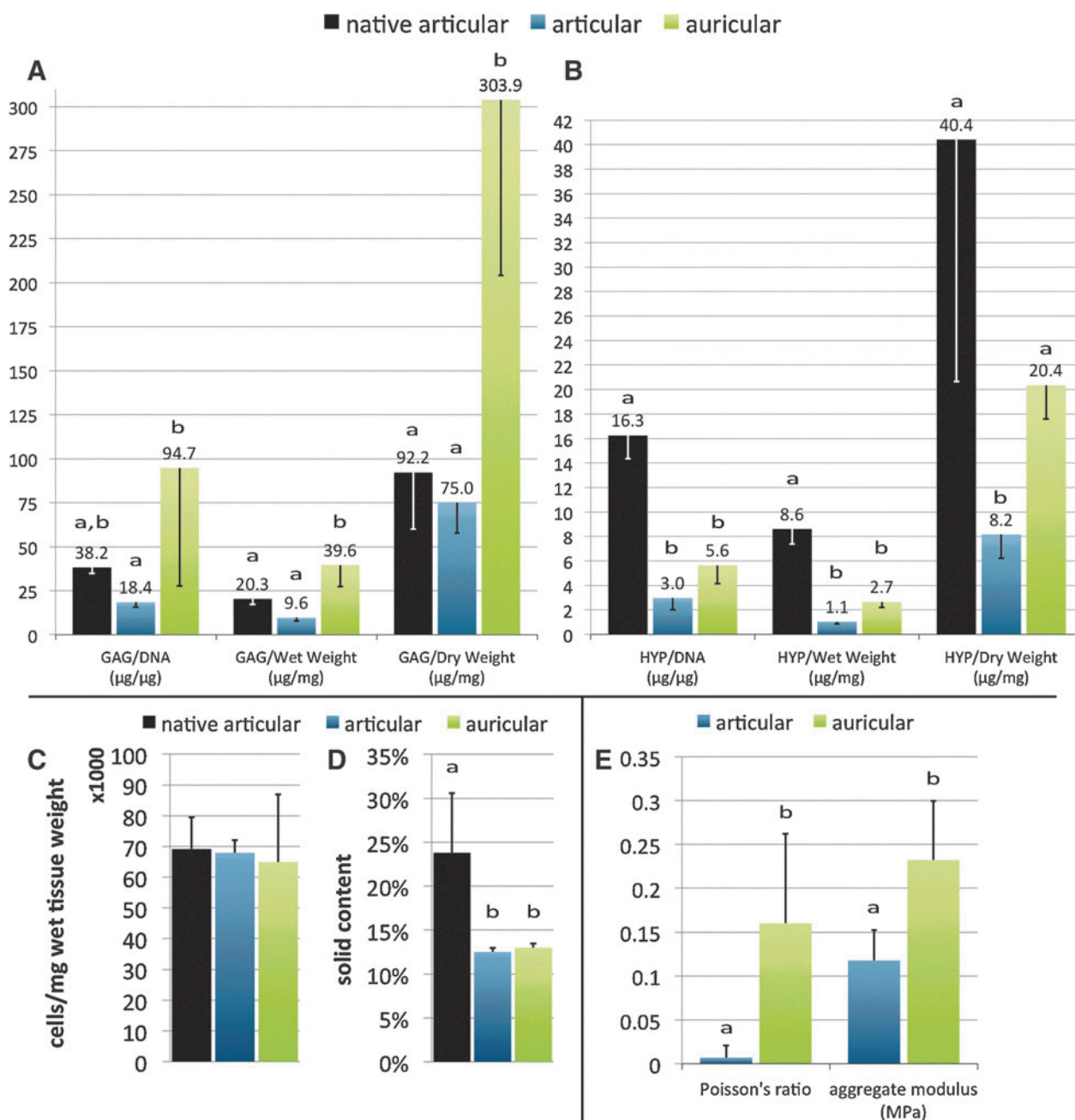


FIG. 5. Biochemical and mechanical characterization. GAG, hydroxyproline (HYP), cellularity, and solid content were measured to characterize tissue composition (A–D). Note the different ranges of the y-axes. The Poisson’s ratio and aggregate modulus were measured for mechanical characterization (E). For both composition and mechanical characterization graphs, letters above each data point indicate statistical comparisons within measured variable groups. Data points which share the same letter are not significantly different, while those that do not share the same letter are significantly different, $p < 0.05$. See the statistical analysis section for number of samples per group.

described here for attaching scaffold-free constructs to porous tantalum was able to produce a construct physically attached to porous tantalum by cellular ingrowth into the pores (Fig. 6C). While integration was successful, the strength of this interface remains to be determined. In this study, auricular chondrocytes were chosen because they produce thicker constructs than articular chondrocytes. As methods are developed to increase the thickness of articular constructs, it is

expected that porous metal integration techniques will be translatable to those constructs as well.

While thickness, mechanical strength, and attachment are potential barriers to clinical application of scaffold-free engineered cartilage constructs for joint resurfacing, in other applications, such as trachea tissue engineering,^{18,19} part or all of these challenges are minimized, significantly lowering the barrier to entry. For example, in cosmetic applications,

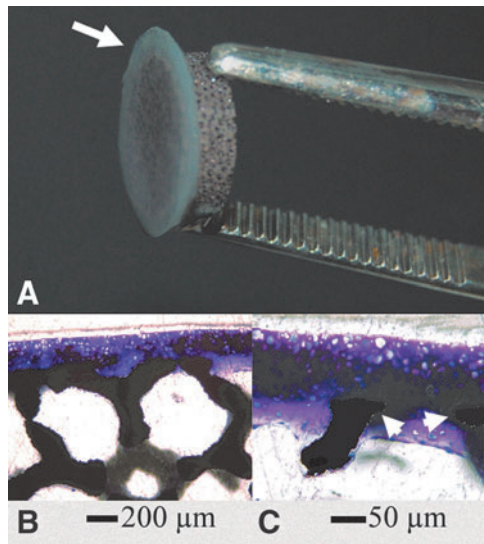


FIG. 6. Porous tantalum integration into scaffold-free cartilage constructs. **(A)** A 1 cm-diameter 4-week tantalum-cartilage composite construct. Cartilage is indicated with an arrow. **(B, C)** Plastic sections stained with toluidine blue. **(C)** is a magnified image of **(B)**, showing cartilage growth around tantalum components (arrowheads), which are pseudo-colored black to increase visibility.

barriers to entry may be much lower, since mechanical properties of constructs as currently generated may be sufficient, and methods for attachment of native cartilage already exist in a variety of plastic surgery applications.^{41,42} We believe that through coordinated and creative approaches, challenges facing arthroplasty applications can be overcome as well.

Conclusion

Scaffold-free engineered cartilage is an attractive approach for cartilage generation because it requires none of the additional materials or methods required for scaffold production and seeding, and eliminates any potentially toxic degradation products. Simple, chemically-defined culture medium differentiation of chondrocytes from skeletally mature populations is possible using the methods described here. In this scaffold-free system, it was found that auricular chondrocytes generated more ECM and produced stiffer constructs than articular chondrocytes. Although auricular constructs appear to have better mechanical properties, both cell types resulted in constructs with stiffness of about one-fourth the reported value for their native counterpart. Additionally, integration of porous metal and scaffold-free constructs is possible.

Acknowledgments

The authors would like to thank Zimmer, Inc., for generously supplying the porous tantalum metal. The project described was supported by Grant AR053622 from NIAMS and NIBIB (J.M.M. and J.E.D.), and by Grant DE015322 from the NIDCR (J.E.D.), and under the Ruth L. Kirschstein National Research Service Award T32 AR007505 from the NIH NIAMS (G.A.W.). The content is solely the responsibility of the authors and does not necessarily represent the official views of the NIDCR, NIBIB, NIAMS, or the NIH.

Author Disclosure Statement

No competing financial interests exist.

References

- Schaefer D, Martin I, Shastri P, et al. *In vitro* generation of osteochondral composites. *Biomaterials*. 2000;24:2599–606.
- Wada Y, Enjo M, Isogai N, et al. Development of bone and cartilage in tissue-engineered human middle phalanx models. *Tissue Eng Part A*. 2009;12:3765–3778.
- Lee M, Siu RK, Ting K, et al. Effect of nell-1 delivery on chondrocyte proliferation and cartilaginous extracellular matrix deposition. *Tissue Eng Part A*. 2010;5:1791–1800.
- Marlovits S, Tichy B, Truppe M, et al. Chondrogenesis of aged human articular cartilage in a scaffold-free bioreactor. *Tissue Eng*. 2003;6:1215–1226.
- Park K, Huang J, Azar F, et al. Scaffold-free, engineered porcine cartilage construct for cartilage defect repair—*in vitro* and *in vivo* study. *Artif Organs*. 2006;8:586–596.
- Lefebvre V, Smits P. Transcriptional control of chondrocyte fate and differentiation. *Birth Defects Res C Embryo Today*. 2005;3:200–212.
- Mainil-Varlet P, Rieser F, Grogan S, et al. Articular cartilage repair using a tissue-engineered cartilage-like implant: an animal study. *Osteoarthr Cartil*. 2001;Supplemental A:S6–S15.
- Jin R, Park S, Choi B, et al. Scaffold-free cartilage fabrication system using passaged porcine chondrocytes and basic fibroblast growth factor. *Tissue Eng Part A*. 2009;8:1887–1895.
- Uenaka K, Imai S, Ando K, et al. Relation of low-intensity pulsed ultrasound to the cell density of scaffold-free cartilage in a high-density static semi-open culture system. *J Orthop Sci*. 2010;6:816–824.
- Stoddart MJ, Ettinger L, Häuselmann HJ. Enhanced matrix synthesis in *de novo*, scaffold free cartilage-like tissue subjected to compression and shear. *Biotechnol Bioeng*. 2006;6:1043–1051.
- Furukawa KS, Imura K, Tateishi T, et al. Scaffold-free cartilage by rotational culture for tissue engineering. *J Biotechnol*. 2008;1:134–145.
- Hoben GM, Athanasiou KA. Creating a spectrum of fibrocartilages through different cell sources and biochemical stimuli. *Biotechnol Bioeng*. 2008;3:587–598.
- Brehm W, Aklin B, Yamashita T, et al. Repair of superficial osteochondral defects with an autologous scaffold-free cartilage construct in a caprine model: implantation method and short-term results. *Osteoarthr Cartil*. 2006;12:1214–1226.
- Grogan SP, Rieser F, Winkelmann V, et al. A static, closed and scaffold-free bioreactor system that permits chondrogenesis *in vitro*. *Osteoarthr Cartil*. 2003;6:403–411.
- Kitahara S, Nakagawa K, Sah RL, et al. *In vivo* maturation of scaffold-free engineered articular cartilage on hydroxyapatite. *Tissue Eng Part A*. 2008;11:1905–1913.
- Nagai T, Sato M, Furukawa KS, et al. Optimization of allograft implantation using scaffold-free chondrocyte plates. *Tissue Eng Part A*. 2008;7:1225–1235.
- Murdoch AD, Grady LM, Ablett MP, et al. Chondrogenic differentiation of human bone marrow stem cells in transwell cultures: generation of scaffold-free cartilage. *Stem Cells*. 2007;11:2786–2796.
- Weidenbecher M, Tucker H, Awadallah A, et al. Fabrication of a neotrachea using engineered cartilage. *Laryngoscope*. 2008;4:593–598.
- Gilpin DA, Weidenbecher MS, Dennis JE. Scaffold-free tissue-engineered cartilage implants for laryngotracheal reconstruction. *Laryngoscope*. 2010;3:612–617.

20. Ryan G, Pandit A, Apatsidis D. Fabrication methods of porous metals for use in orthopaedic applications. *Biomaterials*. 2006;13:2651–2670.
21. Shuler MS, Rooks MD, Roberson JR. Porous tantalum implant in early osteonecrosis of the hip. *J Arthroplasty*. 2007;1:26–31.
22. Levine BR, Sporer S, Poggio RA, et al. Experimental and clinical performance of porous tantalum in orthopedic surgery. *Biomaterials*. 2006;27:4671–4681.
23. Henderson JH, Welter JF, Mansour JM, et al. Cartilage tissue engineering for laryngotracheal reconstruction: comparison of chondrocytes from three anatomic locations in the rabbit. *Tissue Eng*. 2007;4:843–853.
24. Carrino DA, Arias JL, Caplan AI. A spectrophotometric modification of a sensitive densitometric Safranin O assay for glycosaminoglycans. *Biochem Int*. 1991;3:485–495.
25. Ham KD, Oegema TR, Loeser RF, et al. Effects of long-term estrogen replacement therapy on articular cartilage IGFBP-2, IGFBP-3, collagen and proteoglycan levels in ovariectomized cynomolgus monkeys. *Osteoarthr Cartil*. 2004;2:160–168.
26. Woessner JF. The determination of hydroxyproline in tissue and protein samples containing small proportions of this imino acid. *Arch Biochem Biophys*. 1961;2:440–447.
27. Kim YJ, Sah RL, Doong JY, et al. Fluorometric assay of DNA in cartilage explants using Hoechst 33258. *Anal Biochem*. 1988;1:168–176.
28. Mak AF, Lai WM, Mow VC. Biphasic indentation of articular cartilage—I. Theoretical analysis. *J Biomech*. 1987;7:703–714.
29. Mow VC, Gibbs MC, Lai WM, et al. Biphasic indentation of articular cartilage—II. A numerical algorithm and an experimental study. *J Biomech*. 1989;8–9:853–861.
30. Vunjak-Novakovic G, Martin I, Obradovic B, et al. Bioreactor cultivation conditions modulate the composition and mechanical properties of tissue-engineered cartilage. *J Orthop Res*. 1999;1:130–138.
31. Floman Y, Eyre DR, Glimcher MJ. Induction of osteoarthritis in the rabbit knee joint: biochemical studies on the articular cartilage. *Clin Orthop*. 1980;278–286.
32. Setton LA, Mow VC, Muller FJ, et al. Altered structure-function relationships for articular cartilage in human osteoarthritis and an experimental canine model. *Agents Actions Suppl*. 1993;27–48.
33. Sah RL, Yang AS, Chen AC, et al. Physical properties of rabbit articular cartilage after transection of the anterior cruciate ligament. *J Orthop Res*. 1997;2:197–203.
34. LeRoux MA, Arokoski J, Vail TP, et al. Simultaneous changes in the mechanical properties, quantitative collagen organization, and proteoglycan concentration of articular cartilage following canine meniscectomy. *J Orthop Res*. 2000;3:383–392.
35. Chung C, Erickson IE, Mauck RL, et al. Differential behavior of auricular and articular chondrocytes in hyaluronic acid hydrogels. *Tissue Eng Part A*. 2008;7:1121–1131.
36. Naumann A, Dennis JE, Awadallah A, et al. Immunohistochemical and mechanical characterization of cartilage subtypes in rabbit. *J Histochem Cytochem*. 2002;8:1049–1058.
37. Levine B, Della Valle CJ, Jacobs JJ. Applications of porous tantalum in total hip arthroplasty. *J Am Acad Orthop Surg*. 2006;12:646–655.
38. Lima EG, Grace Chao P-h, Ateshian GA, et al. The effect of devitalized trabecular bone on the formation of osteochondral tissue-engineered constructs. *Biomaterials*. 2008;32:4292–4299.
39. Bal BS, Rahaman MN, Jayabalan P, et al. *In vivo* outcomes of tissue-engineered osteochondral grafts. *J Biomed Mater Res B Appl Biomater*. 2010;1:164–174.
40. Ng KW, Lima EG, Bian L, et al. Passaged adult chondrocytes can form engineered cartilage with functional mechanical properties: a canine model. *Tissue Eng Part A*. 2010;3:1041–1051.
41. Ortiz-Monasterio F, Olmedo A, Oscoy LO. The use of cartilage grafts in primary aesthetic rhinoplasty. *Plast Reconstr Surg*. 1981;5:597–605.
42. Brent B. Auricular repair with autogenous rib cartilage grafts: two decades of experience with 600 cases. *Plast Reconstr Surg*. 1992;3:355–374.

Address correspondence to:

G. Adam Whitney, MSc
Hope Heart Matrix Biology Program
Benaroya Research Institute
1201 9th Avenue
Seattle, WA 98101

E-mail: awhitney@benroyaresearch.org